Cyan, magenta and yellow TiO2-based hybrid spheres for electrophoretic inks

Lydia Muentz, Emile Decompte, Hugo Ravet, Nicolas Penin, Anthony Chiron, Cyril Brochon, Georges Hadziioannou, Elodie Bourgeat-Lami, Manuel Gaudon

Materials & Design 258 (2025) 114563

Contents lists available at ScienceDirect

Materials & Design

journal homepage: www.elsevier.com/locate/matdes

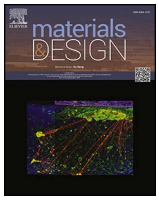

Cyan, magenta and yellow TiO_2-based hybrid spheres for electrophoretic inks

Lydia Muentz [a], Emile Decompte [b], Hugo Ravet [a], Nicolas Penin [a], Anthony Chiron [a], Cyril Brochon [b], Georges Hadziioannou [b], Elodie Bourgeat-Lami [c], Manuel Gaudon [a,*]

[a] Univ. Bordeaux, CNRS, Bordeaux INP, ICMCB, UMR5026, 87 avenue du Dr. A. Schweitzer, F-33608 Pessac, France
[b] Univ. Bordeaux, CNRS, Bordeaux INP, LCPO, UMR5629, Allée Geoffroy Saint Hilaire, Bâtiment B8, F-33607 Pessac, France
[c] Univ. Claude Bernard Lyon 1, CPE Lyon, CNRS, UMR 5128, Catalysis, Polymerization, Processes and Materials (CP2M), 43 Bd du 11 novembre 1918, F-69616 Villeurbanne, France

A B S T R A C T

This study presents an innovative approach for the fabrication of colour electronic inks designed for multi-colour electrophoretic image displays (EPIDs). Hybrid spheres composed of titanium dioxide (TiO_2) cores and organic colourants (cyan, magenta, and yellow), then encapsulated by appropriate polymer shells, were synthesized to be integrated into pixel prototypes for EPIDs. Thus, the work involves three main key steps: (i) the preparation of coloured hybrid spherical particles through spray-drying of TiO_2 suspensions with organic inks, (ii) the exploration and the characterization of the pallet of colourations which are accessible for the hybrid spherical particles, (iii) the enhancement of particle stability in EPID fluids thanks to functionalization (silanisation and polymer encapsulation) and surface charge introduction on the hybrid pigment spheres for stability in apolar media. Electrophoretic performance was evaluated in dual-colour display cells. The hybrid particles demonstrated excellent light-harvesting capabilities and colloidal stability. Electrophoretic tests showed promising performance, with alternating surface colourations and sustained optical contrasts over multiple refresh cycles. This research contributes to the development of advanced colour electronic ink technologies for improved electrophoretic displays.

1. Introduction

The demand for paper like-display devices, with outdoor readability, high reflectivity and contrast, has become crucial for few decades. In this context, ElectroPhoretic Image Displays (EPIDs) have emerged due to their cost-effectiveness, low power consumption, and high flexibility [1,2]. Traditional EPIDs consist of two electrodes enclosing charged particles dispersed in a dielectric fluid, commonly known as electronic ink. When an electric field is applied, the particles migrate toward the oppositely charged electrode, forming an image on the top electrode, which is transparent. Due to the bi-stability of the ink, the image remains visible even in the absence of voltage, with electricity only required for image updates [3]. Despite these advantages, the performance of EPIDs is heavily influenced by several factors, such as particle dispersion stability, high surface charge, and minimal inter-particle interactions [4,5]. Since each pixel typically contains two types of pigments, it is essential that the top layer remains fully opaque to ensure that only the pigment on top is visible, without interference from the pigment underneath. This level of opacity can only be effectively achieved with inorganic pigments.

Currently, most EPIDs are limited to black-and-white displays. Although colour EPIDs have been the subject of theoretical research, they remain far from commercial reality, despite significant progress over the past decade [6–11]. EPIDs can be achieved through two competiting approaches: the use of color filters [12,13], and multi-particle method [14–17]. The color filter strategy is mature but suffers reduced resolution and brightness [14]. In contrast, multi-particle approach could offer the potential for higher visual quality, combining high reflectivity and high contrast. However, two major challenges remain: the way to pilot the different particles move into the apolar solvent, the lack of saturated, non-toxic, and primary coloured inorganic pigments. Ideally, future devices would feature multi-colour pixels, such as white plus three colours or black plus three colours, incorporating primary hues like cyan (C), magenta (M), and yellow (Y), as illustrated in Fig. 1.

First, to implement such as system, four distinct primary particles, with various sizes and charge polarities to enable precise layering each and display precise motion under electric field. Although recent advances – such as dual-charged particle strategy employing white, yellow, black, and red pigments have shown promise, the control of four-

* Corresponding author.
E-mail address: manuel.gaudon@icmcb.cnrs.fr (M. Gaudon).

https://doi.org/10.1016/j.matdes.2025.114563
Received 9 May 2025; Received in revised form 3 August 2025; Accepted 10 August 2025
Available online 11 August 2025

particle EPIDs remains an ongoing technical challenge [14]. In addition, the effectiveness of subtractive mixing depends on the availability of high-performance pigments in cyan, magenta and yellow. While one might assume that a cyan, magenta and yellow primary colours are essential for devices that rely on subtractive colour mixing, and while one might assume that a wide range of inorganic pigments in these colours would be readily available, this is not the case. Contrary to expectations, the range of inorganic pigments capable of producing these essential hues is quite limited. While organic dyes offer a broader array of vibrant CMY colours, inorganic alternatives, particularly for cyan and magenta, are scarce. Unfortunately, molecular dyes suffer from the inherent limitations of organic compounds, such as poor thermal stability and lack of opacity, making them unsuitable for use in EPID inks. Therefore, recent studies continue to explore the development of new, more saturated cyan [18–20], magenta [21–23], and yellow [24–26], inorganic pigments that are also, if possible, non-toxic and free of critical elements. It is interesting to note that the current commercial technologies that include ACeP® and E Ink's Spectra^{TM} try to overcome the issue relying on a "multi-particle" approach in which organic capsules containing cyan-magenta-and yellow organic dyes and TiO_2 inorganic pigment as a white reflector is ensuring color layering [27–29]. However, the control of the white reflector level alongside the organic microcapsules is crucial; it requires complex drive waveforms and push–pull operations associated with high manufacturing costs, long refresh time, particle interferences, and ultimately so moderate display quality.

In addition, EPID inorganic pigments must meet specific requirements: spheroidal particle shapes to prevent irreversible interparticle sticking, particle sizes of less than a few microns with low density to avoid sedimentation, and a minimum size of half a micron to maintain good opacity through efficient Mie Scattering [30–32]. Achieving CMY-coloured inks that meet all these criteria −while also ensuring high charge density in nonpolar media for efficient migration under an electric field − remains a major challenge.

As a preliminary investigation to this study, we aimed to produce spheroidal yellow, cyan and magenta inorganic pigments from $LiCoPO_4$ and $LiNiPO_4$ phosphates using a novel spray-drying method developed in our laboratory [22–33]. These pigments were intended for integration into EPIDs. However, we observed significant colour deterioration after grinding and spray-drying. This prompted us to explore a solution that would preserve the advantages of the inorganic pigments while achieving the colour saturation of organic dyes. This objective guided the present work. In this research, the objective is to demonstrate that micrometer-sized TiO_2 particles (white pigments with high opacity) spherodized via spray drying and incorporating cyan, magenta, and yellow dyes on their surface, could be widely served in the near future as viable alternative to commercial inorganic pigments, which often suffer from limited coloration properties and/or toxicity issues, in electrophoretic inks using the 'multi-particle' approach. A proof-of-concept will be conducted on dual-charged macropixels to assess the viability of this strategy.

In details, we investigate the use of commercially available Epson printer molecular dyes to create cyan, magenta, and yellow inorganic–organic composite inks. These inks are produced through co-spray-drying with TiO_2 suspensions, resulting in hybrid particles. To optimize the colour contrast and performance of the resulting pigments, we used UV–visible (UV–vis) spectroscopy, a reliable method for precise colour evaluation. This technique allowed us the analysis of the interactions between the dye and dispersing medium, and compare the stability of pigments and hybrid pigments under various conditions. Additionally, to reduce the apparent density of the pigments − an essential factor for efficient displays − the hybrid particles were encapsulated in a poly (methyl methacrylate) (PMMA) shell and functionalized with surface charges, making them suitable for use in EPIDs. Finally, we demonstrate the practical application of these hybrid inks in a working EPID, advancing the development of colour-changing display technology by combining precise spectroscopic analysis and innovative particle functionalization.

2. Experimental

2.1. Powder preparation

The synthesis of hybrid spherical particles was carried out using a Büchi Nano Spray Dryer B-90, set at 120 °C, and equipped with a 4.0 µm mesh spray cap (Fig. 2). The spray dryer operated in an open-loop configuration, using compressed air as the drying gas at around 120 mbar. The process typically lasted around two hours, producing between 100 and 1500 mg of powder. The goal was to produce submicron TiO_2-based spheres that encapsulate molecular inks to provide colour. The dyes used were commercial printer inks − cyan, yellow, and magenta - from the Epson® EcoTank 105 series. The TiO_2 nanopowder selected was an Aeroxide® P25 anatase/rutile mixture, which offers the advantage of easy dispersion in aqueous solution as small aggregates of a

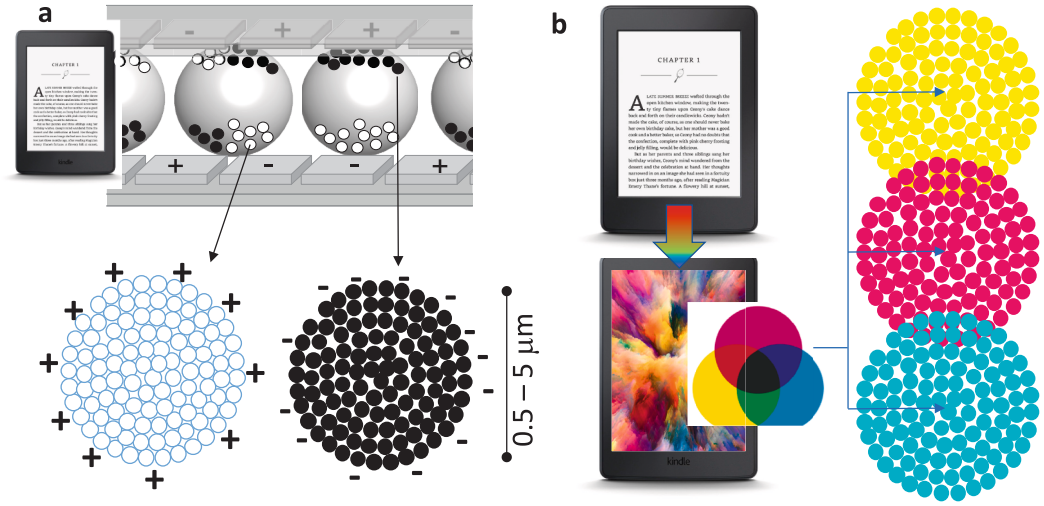

Fig. 1. A) cross-sectional view of a traditional electrophoretic display, where pixels are composed of black and white inorganic pigments in spherical aggregates. b) potentialities of a full-colour display with 4-particle approach,i.e. with the addition of cyan, magenta, and yellow spherical aggregates within white or black microcapsules.

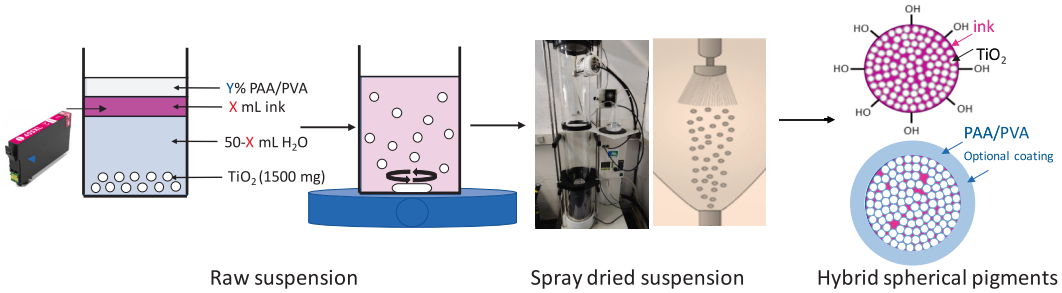

Fig. 2. Preparation route for TiO_2-based hybrid pigments starting from a suspension of TiO_2 particles, coloured ink (Epson-Magenta ink), water as the solvent, and PVA or PAA polymer as a dispersant/stabilizer, followed by spray-drying.

few tens of nanometres.

To produce the "hybrid spherical pigments", the first step involved creating a suspension of TiO_2 nanoparticles in a solution of dye, water, and optionally a polymer such as polyacrylic acid (PAA) or polyvinyl alcohol (PVA). These polymers were added to help stabilize the organic C, M or Y ink within the hybrid pigments. The suspension was stirred with a magnetic stir bar for 30 min to ensure uniform dispersion prior to spray-drying, with continuous stirring maintained throughout the spray-drying process.

During spray-drying, the suspension was atomized into droplets using the mesh spray cap, through which the suspension was pumped. These droplets were then quickly dried in a drying cylinder under controlled pressure and heated airflow. The resulting dry powder was collected by generating an electric field between a high-voltage electrode and a collecting electrode, housed in a large metal tube at the base of the system. Finally, the powder was retrieved by scraping the inside of the collecting electrode with a specialized spatula.

The hybrid spherical pigments produced are named according to their colour (C, M, or Y) and the volume of ink used (X). For instance, a suspension was prepared by combining 2 mL of cyan dye, 48 mL of water, and 1.50 g (about 3 wt%) of TiO_2. In this case, the sample would be labelled as C-2, indicating a cyan hybrid pigment containing 2 mL of ink.

2.2. Stability tests in Isopar G

To assess the stability of the organic C/M/Y inks contained within the hybrid spherical pigments in Isopar G (the standard dispersive medium for EPID inks), both with and without polymer, 50 mg of the pigment was added to 5 mL of Isopar G. The mixture was then heated to 120 °C with magnetic stirring for 2 days. Afterward, the pigments were left to rest in a test tube for an additional 2.5 months. Photos were taken during the tests to monitor any potential loss of colour into the medium or any change in the colour of the sample.

2.3. Particle silanisation

Silanisation was performed only on the hybrid spherical pigments without PAA or PVA protective shells. Before being encapsulated with PMMA, the hybrid spherical pigments were functionalized *via* silanisation to introduce free double bonds on their surface. As an example, 200 mg of hybrid spherical particles was mixed with 10 mL of toluene and 0.3 mL of trimethoxysilyl propyl methacrylate (TPM) in a 25 mL round-bottom flask. The mixture was sonicated for 30 min to ensure proper dispersion of the particles in the apolar solvent. The flask was then connected to a condenser and placed in an oil bath preheated to 120 °C, where it was magnetically stirred at 500 rpm for 17 h. Afterward, the resulting dispersion was purified by centrifugation/redispersion cycles in fresh toluene to remove any unreacted species. The functionalized hybrid spherical particles were then dried in a vacuum oven at 40 °C overnight (Fig. 3).

2.4. Particle encapsulation

The functionalized hybrid pigments were encapsulated using dispersion nitroxide-mediated polymerization (NMP) in an apolar media, specifically isoparaffin G. Dispersion polymerization is a heterogeneous technique in which the monomer is initially soluble in the continuous phase, but the growing polymer chains become insoluble and precipitate to form colloidal particles stabilized by dispersants. First, a poly-lauryl acrylate (PLA) macroinitiator based on the SG1-based alkoxyamine BlocBuilder® was synthesized (Fig. 3). Typically, 10 g of lauryl acrylate (LA) and 0.2 g of BlocBuilder® were mixed with 10 mL of toluene in a 50 mL one-neck round-bottom flask, which was then sealed with a septum. The mixture was degassed by bubbling argon for 30 min in an ice bath under magnetic stirring (400 rpm). The polymerization was carried out at 120 °C and 500 rpm in an oil bath for at least 17 h. The resulting polymer was recovered by successive precipitation in cold methanol, and the transparent viscous liquid was then dried under vacuum at 50 °C for 24 h. Next, using the alkoxyamine-terminated macroinitiator, a second polymerization was conducted in the presence of the hybrid spherical pigments. To this end, 200 mg of TPM-

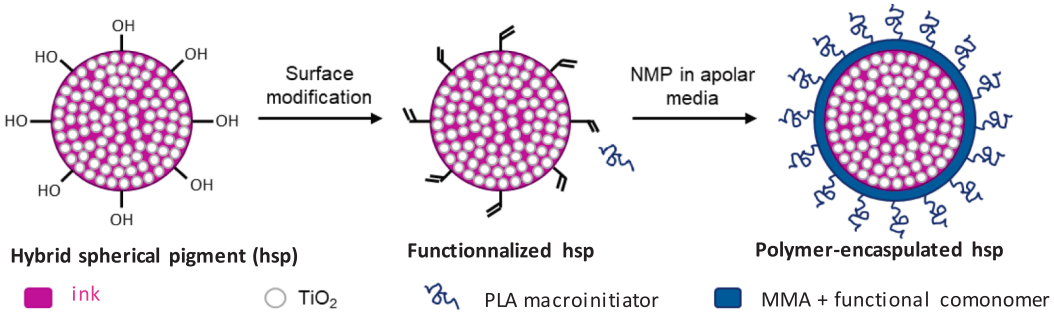

Fig. 3. Schematic representation of the encapsulation process for the hybrid spherical pigment.

functionalized particles were mixed with 250 mg of macroinitiator and 8 mL of Isopar G. The mixture was sonicated for 30 min to aid in the dispersion of the inorganic particles. Then, a mixture of methylmethacrylate (MMA) and either acrylic acid (AA) to impart negative charges or 2-dimethylaminoethyl methacrylate (DMAEMA) to provide positive charges, was added. Argon was then bubbled through the mixture for 30 min to remove oxygen, while maintaining the system in an ice bath under magnetic stirring (400 rpm). The flask was then immersed in a preheated oil bath at 120 °C and 500 rpm for 16 h to complete the polymerization. Finally, the encapsulated particles were purified through multiple centrifugation/dispersion cycles until the supernatant became transparent indicating the absence of free latex particles. The final electrophoretic particles (encapsulated hybrid spherical pigments) were dried overnight under vacuum at 40 °C.

2.5. Scanning Electron Microscopy (SEM)

The atomized powders were characterized by SEM to assess their morphology and granulometry. The analysis was performed using a Quanta 3D FEG SEM, at an acceleration voltage of 5 kV. Granulometric analysis was carried out with ImageJ software, where the diameter of each particle was manually measured by marking coordinates on the image. The data were then exported for further analysis.

UV − visible − Near InfraRed (UV–vis-NIR) diffuse reflectance spectra were recorded at room temperature from 200 to 2500 nm with a 1 nm step and a 2 nm bandwidth, using a Cary 17 spectrophotometer equipped with an integration sphere. Halon polymer served as the white reference for the blank. The spectra obtained were mathematical processed to determine the L*a*b* colourimetry parameters, where L* represents lightness, a* corresponds to the green-to-red axis, and b* represents the blue-to-yellow axis [34]. Colour squares, visually illustrating the pigment colouration, were generated from the L*a*b* parameters using the free software easyRGB (https://www.easyrgb.com/en/), and the associated RGB colourimetry parameters were then managed using PowerPoint (Microsoft Pack Office). To determine the color difference (ΔE) between two colours (1 and 2), the distance between their respective points in the CIELab colour space was calculated using the eq. ().

$$\Delta E = \sqrt{(L_1 - L_2)^2 + (a_1 - a_2)^2 + (b_1 - b_2)^2} \quad (1)$$

Additionally, the Kubelka − Munk transformation was applied to the visible diffuse reflectance spectra R(λ) to calculate the absorption coefficient K and scattering coefficient S of the sample, using the eq. (2).

$K/S = (1 - R)^2/2R$ **(2)**

These coefficients were then used in mixing laws.

2.6. Turbiscan stability index (TSI) measurements

The stability of the inks was evaluated using a Turbiscan-Lab Stability Analyzer, which tracks the stability of colloidal dispersions over time by measuring the transmittance and back-scattering ratios of a pulsed near-infrared light (λ = 880 nm). The TSI is determined by analysing the time evolution of the transmission of each suspension layer at different heights (h) and normalizing the results by the total analysed thickness (H), providing a value independent of the sample quantity in the measuring tube.

2.7. Pixel prototype

The optical properties of the electrophoretic inks were investigated using a testing device that consisted of an iron bottom electrode and an ITO glass top electrode, separated by a Teflon spacer (~ 500 μm). An electric field (E = 0.36 V·μm^{-1}) was applied to induce particle movement, and the resulting colour change was observed through the transparent ITO top electrode, from UV–visible diffuse reflectance spectroscopy.

3. Results

3.1. Formation of spheroidal TiO_2-based hybrid pigments by Spray-Drying

The initial studies focused on investigating the impact of TiO_2 content in the aqueous suspension on the size and size distribution of the final beads after spray drying, in the absence of dye (Fig. 4). SEM results showed that as the TiO_2 concentration increased, the sphere size also increased. Since the size of the atomized droplets remains constant (determined by the membrane's pore size), the ratio between droplet size and TiO_2 sphere size after drying is directly influenced by the amount of TiO_2 introduced. Consequently, the sphere volume should show a linear correlation with TiO_2 content, and the diameter should be proportional to the cube root of this value. Particle size distribution analysis confirmed this trend (Fig. 7**a,b,c**). Specifically, mean diameters increased from 1.21 μm at 1 wt% TiO_2 to 1.77 μm at 3 wt%, and 2.22 μm at 10 wt%.

As the TiO_2 content in the sprayed suspensions increased, the spherical particles became smoother and better defined. According to the specifications for electrophoretic inks, which require pigments of micrometric size to ensure efficient scattering and opacity, the particle sizes obtained with the suspension containing only 1 wt% TiO_2 (approximately 1 μm) are the most suitable. However, producing in a single day only about 100 mg of powder at such low concentration is inefficient. Since the quantity of droplets generated per unit of time is constant, the powder mass produced increases linearly with TiO_2 content. As a result, further studies will use 3 wt% TiO_2 suspensions as a compromise.

We then studied the impact of dye addition on the morphology of the hybrid spheres for 3 wt% TiO_2. The effect of introducing molecular dyes, yellow and magenta, into the suspension was investigated by adding 5 mL of ink to the raw suspension (see SEM micrographs in Fig. 5). Notably, the molecular dye is not visible in the SEM images. The images show that the addition of the dye had no discernible effect on particle morphology. Additionally, size distribution analysis of the three batches—TiO_2, TiO_2 with yellow dye, and TiO_2 with magenta dye—revealed no significant differences in particle size (see Fig. 7**a,f,**g).

With the goal of forming a protective polymer shell around the polycrystalline TiO_2 spheres to prevent the dye molecules from being released into the electrophoretic dispersion medium during ageing, the synthesis was repeated by adding two water-soluble polymers, PAA and PVA. As both polymers gave similar results, only PVA is presented here. SEM micrographs in Fig. 6 illustrate the results for different PVA/TiO_2 weight ratios (0, 0.25 and 0.5). The addition of PVA produced two distinct effects as its concentration increased: (i) a deformation of the particles, with the shape transitioning from well-defined specular shape to "donut" shapes, and (ii) an increase in characteristic diameter, from 1.21 μm (with no PVA) to 1.34 μm (at 25 wt% PVA) and 1.59 μm (at 50 wt% PVA). The diameter distribution also widened, particularly for the 50/50 ratio (Fig. 7**a,d,e**). The evolution of the characteristic diameter is influenced by the PVA/TiO_2 weight ratio. Changes in the average diameter can provide insights into whether the PVA fills the pores of the polycrystalline TiO_2 spheres before forming a shell around them, or if it simply forms a shell. Using the diameter of TiO_2 spheres without PVA (1.21 μm) as a reference and considering that the TiO_2 spheres are porous (with approximately 45 % density), we can calculate the predicted characteristic diameters at 25 wt% and 50 wt% PVA based on two different hypotheses. First, mass percentages are converted to volume percentages using the following equation: PVA (vol%) = PVA (wt%) / [(PVA (wt%) + $\rho_{(PVA)}$ / $\rho_{(TiO2)}$ × (1-PVA (wt%))], with $\rho_{(PVA)}$ = 1.27 g cm^{-3} and $\rho_{(TiO2)}$ = 4.26 g cm^{-3}. This results in 53 vol% PVA for 25 wt% and 77 vol% PVA for 50 wt%. If all the PVA forms a shell, the average diameter of the PVA-coated hybrid spheres is calculated as 1.42 μm for

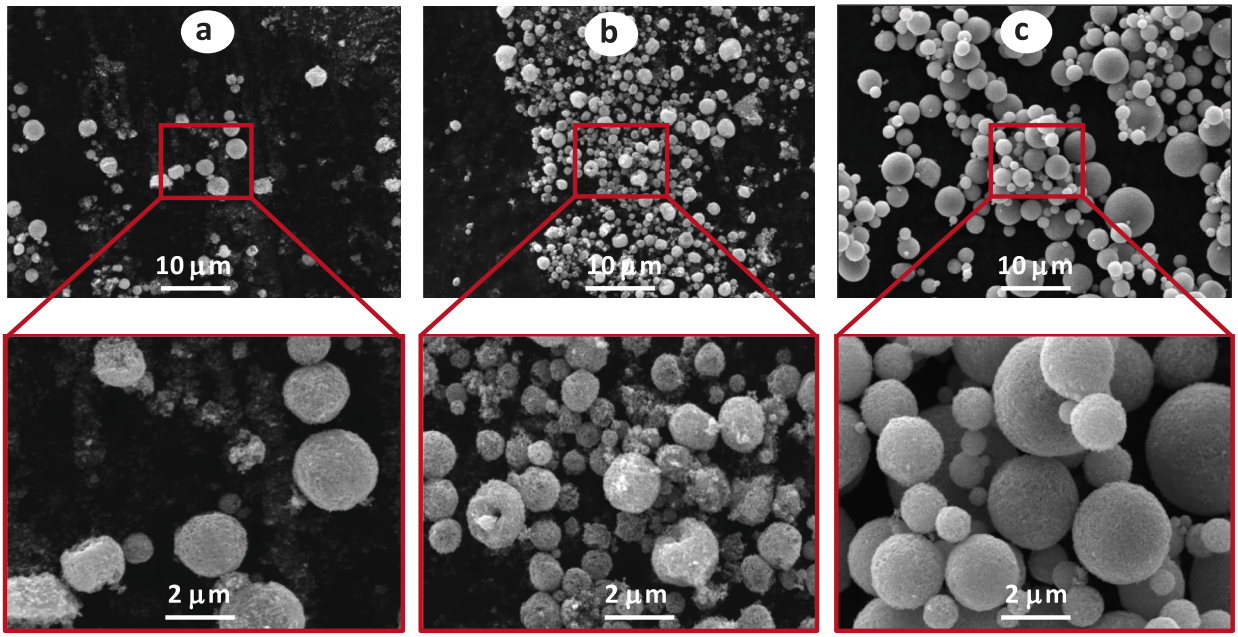

Fig. 4. Spray-dried spheres obtained from TiO_2 suspensions (without polymer or ink) for increasing TiO_2 contents: 1 wt% (a), 3 wt% (b), and 10 wt% (c).

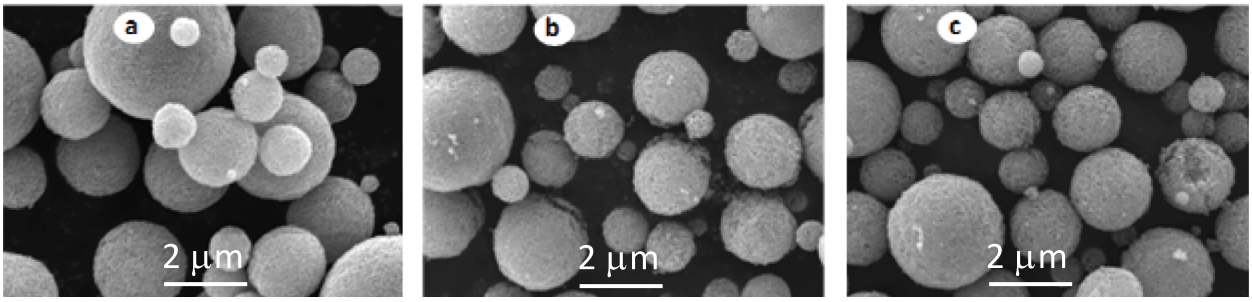

Fig. 5. Spray-dried spheres obtained from 3 wt% TiO_2 suspensions without any dye (a), with the yellow ink (b), and with the magenta ink (c) (X = 5 mL).

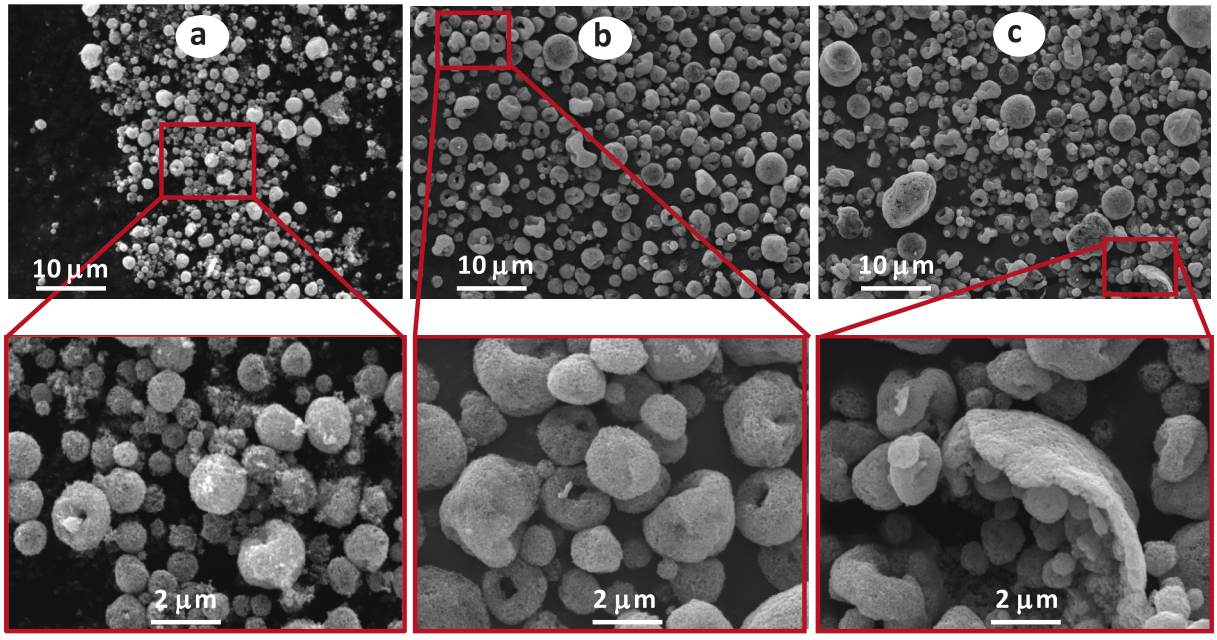

Fig. 6. Spray-dried spheres obtained from 3 wt% TiO_2 suspensions and PVA polymer at different PVA/TiO_2 weight ratios: 0/100 (a), 25/75 (b), and 50/50 (c).

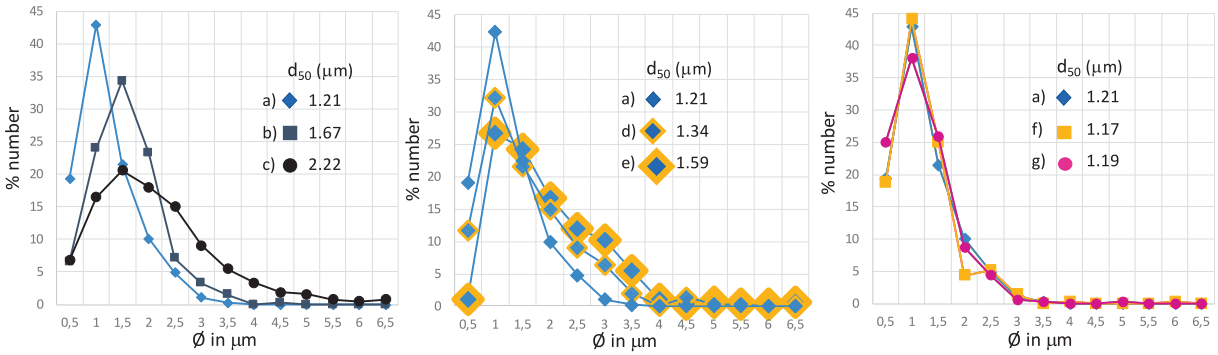

Fig. 7. Particle size distribution of all the atomized spheres obtained in this study starting from pure TiO_2 suspensions: a) 1 wt%, b) 3 wt% and c) 10 wt%; from 3 wt % TiO_2/PVA suspensions: d) PVA/TiO_2 (wt/wt) = 25/75, and e) PVA/TiO_2 (wt/wt) = 50/50; and from 3 wt% TiO_2/dye suspensions: f) yellow dye and g) magenta dye (X = 5 mL).

the 25/75 ratio and 1.71 µm for the 50/50 ratio. If a fraction of the PVA is consumed to fill the pores of the TiO_2 spheres, the average diameter of the PVA-coated hybrid spheres is calculated as 1.24 µm for the 25/75 ratio and 1.59 µm for the 50/50 ratio. The experimental values fall between these two sets of calculations, indicating that the PVA likely distributes between filling the intra-spherical porosity and forming a surface shell. Initially, the PVA fills the internal pores of the TiO_2 agglomerates, and with increasing PVA content, a polymer shell progressively develops around the spheres.

While not intended as formal aging tests, these preliminary experiments indicate that the hybrid pigments display good colloidal stability and exceptional colour retention under the tested conditions. We then tested the colour stability of the organic dyes, which provides colour to the hybrid pigment spheres, both with and without an additional PVA shell, when dispersed in a standard electrophoretic solvent. The colour stability was evaluated using magenta dye at varying PVA concentrations (0 wt%, 25 wt%, and 50 wt%), after dispersion via sonication in Isopar G.

Turbiscan Lab Stability Analyzer was used to determine the TSI, which gives insight into the sedimentation rate, with lower TSI values indicating higher colloidal stability. The results, including photographs taken after 4 months of ageing (at room temperature, in daylight, and about 55 % humidity), are reported in Fig. 8. These preliminary experiments, which are not intended to serve as actual aging tests, indicate an apparent exceptional stability of the organic dyes. This result is particularly notable given the use of a multiphasic TiO_2 substrate (anatase and rutile), well known for its photocatalytic activity [35,36]. It is highly likely that the immersion in the dispersion medium – Isopar G, a transparent and non-polar solvent with significant UV absorption in its spectral range – contributes substantially to this observed stability [37].

Contrary to expectations, the addition of PVA did not enhance the stability of the hybrid particles in Isopar G. Instead, it led to increased sedimentation, as indicated by the TSI curves over time. The most stable ink was obtained with 0 % PVA, while the formulation with 25 wt% PVA exhibited the lowest colloidal stability. The ink with 50 wt% PVA showed intermediate behaviour. In agreement with the previous calculations, these findings suggest that PVA does not simply form a distinct shell around the TiO_2 spheres. Instead, it appears to fill the internal porosity of the aggregated polycrystalline spheres. By replacing Isopar G (density ~ 0.755 g cm^{-3}) with PVA (density ~ 1.19 g cm^{-3}) in the intragranular spaces, the particle mass increases, promoting sedimentation. This effect is particularly pronounced for the sample with 25 % PVA, where the majority of the PVA is used to fill the intra-sphere pores, thereby increasing the overall density. However, as the amount of PVA increases further, the density begins to decrease again, since PVA is less dense than TiO_2 and no longer contribute to filling the pores beyond a certain point.

As shown in the photographs, after 15 days of immersion in Isopar G, the particles remained fully coloured regardless of the PVA content, while the solvent stayed colourless, indicating no leaching of the organic molecules. In particular, no visual degradation of colour was observed, even after up to four months. The organic molecules in the Epson inks appear to interact effectively with the inorganic TiO_2 nanoparticles, physically trapping the dye within the hybrid particles, and ensuring colour stability in Isopar G. Therefore, for the next studies, the optimization of the colourimetry properties will focus solely on the hybrid pigment spheres composed of the inorganic core and the molecular ink, without any PVA addition.

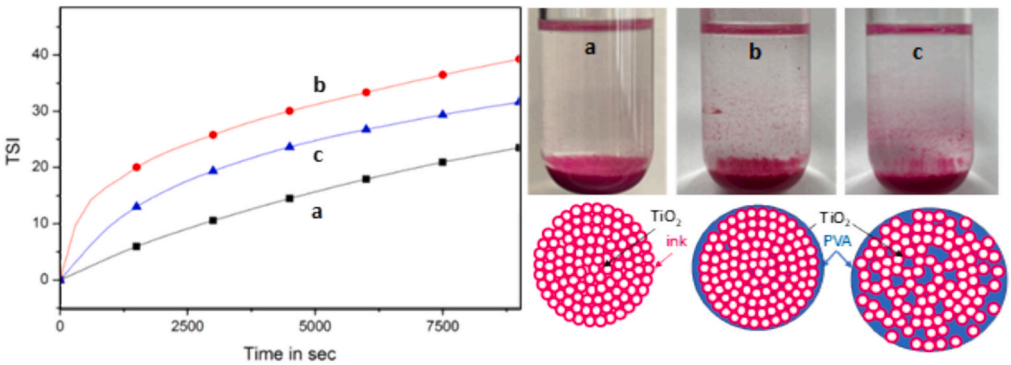

Fig. 8. TSI measurements, photographs of dispersions in isopar G (after 15 days of ageing), and schematic representations of the morphology of PVA/TiO_2/magenta ink hybrid spheres with different PVA/TiO_2 weight ratios: 0/100 (a), 25/75 (b), and 50/50 (c).

3.2. Colouration properties of the hybrid pigments

The colouration of the hybrid pigments was studied on the powders obtained after spray-drying, using diffuse reflection on a powder bed. The spectra are accompanied by coloured squares representing the most accurate colour for each sample, based on the L*, a*, b* parameters extracted from UV–vis spectra. Additionally, the color difference (ΔE) between the observed colour and the corresponding ideal colour inks was also reported to assess colour fidelity (Fig. 9).

In a first study, we examined the effect of the volume of Epson ink added to the starting suspensions on the colouration of the resulting powders. The tests were conducted with magenta and yellow inks, with Epson ink volumes varying from 1 to 10 mL. The results, shown in Fig. 9, include the samples M−1, M−2, M−5, M10, Y-1, Y-2, Y-5 and Y-10. For magenta, the optimal colour was achieved with 2 mL of ink, resulting in the closest match to the ideal magenta (i.e., the lowest color difference) (M−2 in Fig. 9**a**). Similar results were obtained for yellow ink (**Figure** b), and it is anticipated that the same trend would apply to cyan ink.

Secondly, we aimed to demonstrate that mixing magenta and yellow inks could yield red pigments. Two 50/50 wt/wt mixtures were prepared. First, by combining the inks in suspension before spray-drying: 1 mL of each magenta and yellow ink was added to the raw suspension, totalling 2 mL of ink (referred to as ink mixtures). Second, by mixing the magenta (M−2) and yellow (Y-2) atomized powders in a 50/50 wt ratio using a mortar and pestle (referred to as powder mixtures). Both methods were expected to produce similar colours, which could be predicted from the colours of the Y-2 and M−2 pigments using 2-flux models. Two models are proposed here. The Duncan law (eq. 3) was applied to model the mixing of the powders after spray-drying, assuming the scattering factor (S) is identical for both powders, thus simplifying the equation. This assumption is based on the scattering factor being primarily derived from the base TiO_2 refractive index, while the organic dyes contribute negligible scattering efficiency [38,39]. An alternative equation was used to represent the mixing of dyes on a white support (eq. 4) [40]. The two equations produced only slightly different predictions (Fig. 10**a**). However, the experimental results led to significantly different colourations for the ink and powder mixtures (Fig. 10**b**). The reason for the disparity between the two mixing procedures is unclear. One possible explanation is multi-scattering as both methods rely on a two-flux model that considers only single scattering. The scattering interactions involving the yellow or magenta dye may not be fully captured in these models. Additionally, it is worth noting that the resulting red colouration, regardless of the sample preparation method, is somewhat distant from the ideal red. This can be attributed to the mismatch between the starting yellow and magenta inks and their ideal counterparts, rather than an issue with the experimental mixing of the hybrid spheres. Indeed, the predicted red colourations based on Duncan's model or the dyes-on-white substrate law show a similar, if not slightly greater, deviation from the ideal red.

Eq. (3) Simplified Duncan's law for mixing equal parts (50 wt% each) of magenta (M−2) and yellow (Y-2) hybrid spheres. *K* and *S* are absorption and scattering coefficient, respectively.

$$\left(\frac{K}{S}\right)_m = \left(\frac{K}{S}\right)_{support} + \sum_i \frac{K_i}{S_i} \rightarrow \left(\frac{K}{S}\right)_{support} + \left(\frac{K}{S}\right)_{M,1mL} + \left(\frac{K}{S}\right)_{Y,1mL} = \left(\frac{K}{S}\right)_{M,1mL} + \left(\frac{K}{S}\right)_{Y,1mL}$$

Eq. (4) Equation for mixing magenta and yellow dyes (1 mL each) on a white TiO_2 support. *K* and *S* are absorption and scattering coefficient, respectively.

$$\left(\frac{K}{S}\right)_m = \sum_i \frac{K_i{}^*C\%}{S_i{}^*C\%} = \frac{K_{M-2}{}^*0.5 + K_{Y-2}{}^*0.5}{S_{M-2}{}^*0.5 + S_{Y-2}{}^*0.5} = \frac{K_{M-2}{}^*0.5}{S} + \frac{K_{Y-2}{}^*0.5}{S}$$

Building on the above results, which demonstrated that a red colour could be produced by mixing yellow and magenta hybrid pigment spheres, we extended the study to the creation of green and blue. Each sample was prepared as a 50/50 powder mixture of the corresponding C/M/Y-2 pigments (Fig. 11**b**, with the C-2 spectrum also shown in Fig. 11**a**). The ΔE color difference between the prepared red, green, and blue powders and their ideal counterparts is reported and compared. It can be seen that creating green and blue pigments by mixing magenta and cyan hybrid spheres is more challenging than producing the red colour. Nevertheless, a very wide palette of colours can be quickly achieved.

In any case, the hybrid particles developed in this study offer the potential to generate a broad range of colours, which would be challenging to achieve with conventional inorganic inks. As a result, the final phase of the study focused on developing a prototype pixel for EPIDs, incorporating two pigments. Thanks to the synergistic combination of the highly reflective inorganic core of the hybrid particles and the embedding of organic dyes, the six primary colours tested as a proof of concept yield electro-addressable pigments with remarkable potential performance in an electrophoretic ink. The corresponding colorimetric parameters and their positions on the x-y colour map are presented in Fig. 12.

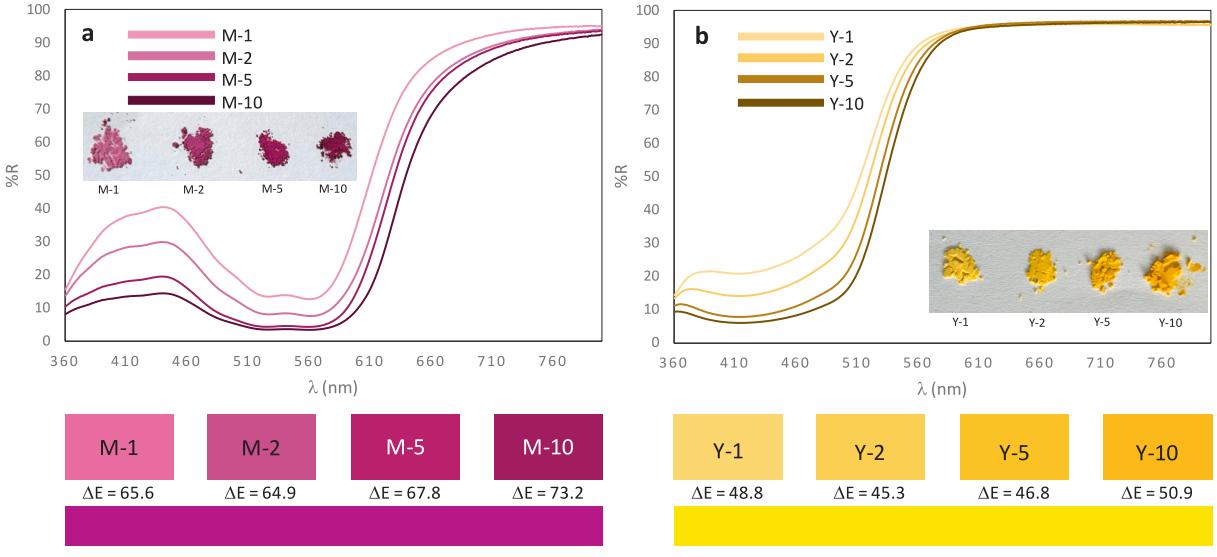

Fig. 9. Diffuse reflection spectra of a) magenta and b) yellow hybrid spheres with varying ink amounts (X = 1, 2, 5 or 10 mL, respectively).

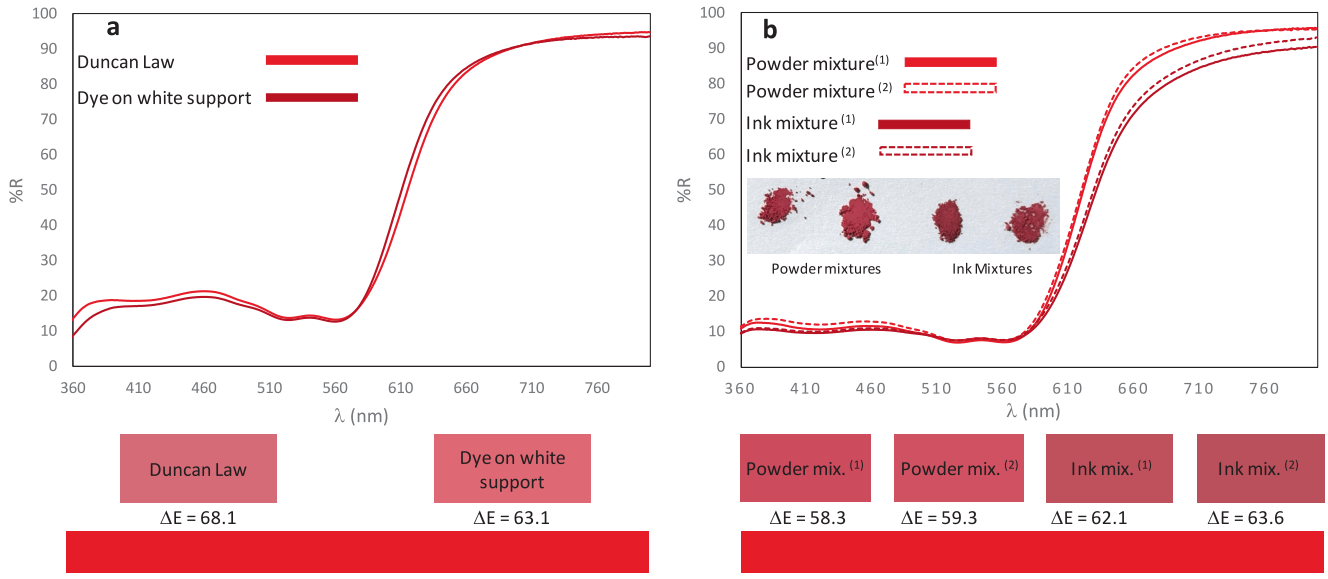

Fig. 10. A) calculated diffuse reflection spectra based on duncan's law or the dye-on-white support law for a 50/50 (wt/wt) mixture of magenta and yellow hybrid spheres, compared with b) experimental diffuse reflection spectra from two samples prepared with either a 50/50 (wt/wt) mixture of magenta and yellow hybrid powders or with equal parts (50 wt% each) of magenta and yellow inks introduced in the TiO_2 suspension prior to spray-drying. (1) and (2) correspond to the same experiment repeated twice.

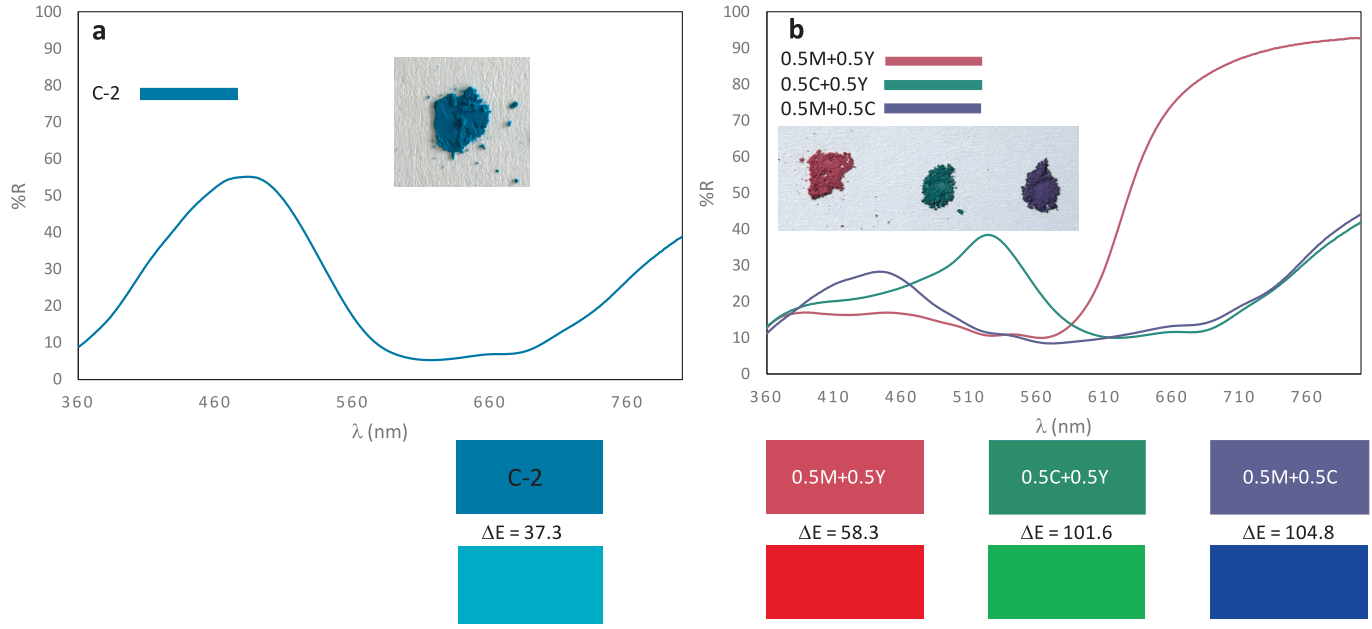

Fig. 11. A) diffuse reflection spectra of cyan (x = 2 mL) hybrid spheres and b) tests for preparing the three red, green, and blue primers from blends of magenta, cyan and yellow powders in 50/50 (wt/wt) proportions.

3.3. Pigment modification encapsulation for electrophoretic ink

Each inorganic pigment was modified to provide the stability for controlled particle motion under an applied electric field as schematically represented in Fig. 3. The general procedure has been already described in previous work [41].

First, a surface modification was carried out via silanisation using TPM to promote polymer anchoring. This functionalization facilitates pigment dispersion in organic media and enables the formation of a stable polymer shell during dispersion polymerization. Following this step, a polymer coating was applied. This coating serves three essential functions: (1) it renders the particles compatible with the dielectric solvent by introducing a hydrophobic surface; (2) it induces steric repulsion and reduces particle density to prevent aggregation and sedimentation; and (3) it imparts surface charges, enabling electrophoretic mobility. To do so, the modified particles were dispersed in Isopar G along with the PLA macroalkoxyamine initiator, MMA, and the appropriate functional monomers—either AA or DMAEMA—to introduce surface charges into the polymer shell. Dispersion polymerization was subsequently carried out, resulting in particles stabilized by PLA chains grafted onto their surface (see Fig. 3). Surface charges were generated through acid–base interactions between the functional monomers: carboxylic acid groups from AA units provide negative charges (carboxylates), while tertiary amine groups from DMAEMA yield positive charges (ammonium ions), as previously reported [42].

		R-G-B	x - y
C-2		0-163-194	0.21 - 0.28
M-2		196-79-148	0.38 - 0.24
Y-2		255-222-89	0.42 - 0.46
R = 0.5 M+0.5 Y		101-93-117	0.48 - 0.30
G = 0.5 C+0.5 Y		58-157-115	0.28 - 0.41
B = 0.5 C+0.5 M		100-98-148	0.26 - 0.23

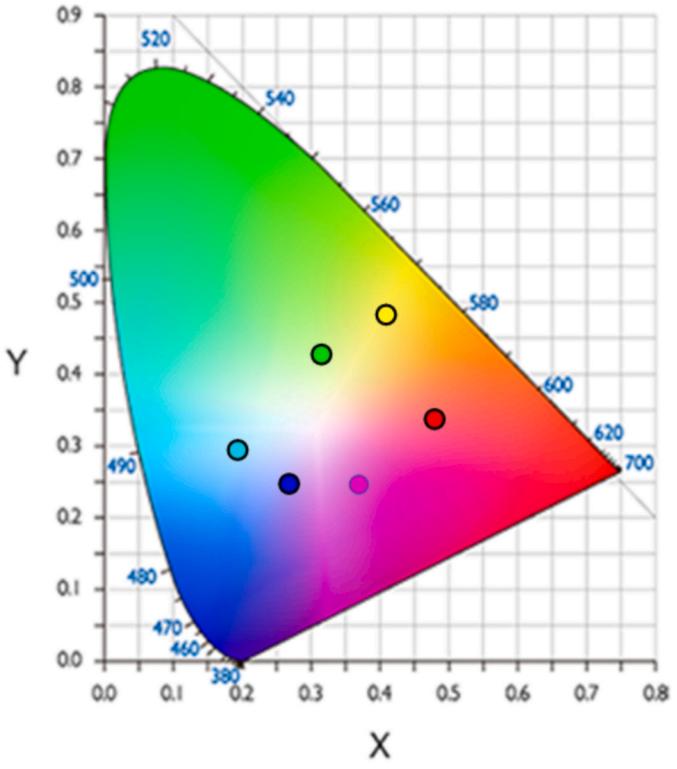

Fig. 12. In a glimpse, RGB (0–255) colorimetric parameters, associated x,y coordinates and their positioning on xy colour map of the six primary-colour samples as-prepared.

3.4. *Testing ink performance in an electrophoretic display*

Two binary colour dispersions were tested in an electrophoretic test cell (dual-colour display) to evaluate the generated by the migration of oppositely charged hybrid particles to the viewing surface. An apolar solvent was used as the electrophoretic medium to suppress ionic conductivity and prevent current leakage [43–45]. The first dispersion contained a spheroidised TiO_2 white pigment (without ink), and a red hybrid pigment sphere, selected from one of the red pigments prepared by mixing 50 % magenta and 50 % yellow inks in a single atomized suspension. The second dispersion contained two types of hybrid spheres: one loaded with magenta pigment and the other with yellow pigment.

In the final electrophoretic dispersions, the particles were mixed with the following weight ratios: white/red = 1:4 and yellow/magenta = 1:2. The corresponding charge characteristics were as follows: negatively charged white particles, negatively charged yellow particles, and positively charged red particles. (Fig. 13**)** [46].

The electrophoretic test cell consists of two electrodes: a transparent electrode on top (ITO glass: i.e. a borosilicate glass coated with a conductive indium-doped tin oxide thin film) and a reflective electrode on the bottom (metal). After introducing the inks into the device's prototypic pixel, a potential difference of ± 180 V was applied (Fig. 14**a**). For the white/red ink, the negatively charged white particles migrated to the top electrode under a positive voltage (Fig. 14**b**), whereas the red particles migrate upward to the top electrode when a negative voltage is applied (Fig. 14**c**). A clear ΔE colour difference was observed between the two states. As demonstrated in the Supplementary Video (**R-W_protopixel.mov**), the contrast between red and white can be switched repeatedly without visible degradation. Full refreshes of both colour states were achieved simply by reversing the polarity of the applied potential. Although this video is not sufficient to assess long-term bistability or cycling durability. It already illustrates the potential for fast switching cycles – seven full cycles are completed in approximately twelve seconds – thereby showing performance levels (in terms of response and refresh rates) that are fully comparable to recent high-performance electrophoretic inks based on commercial inorganic pigments [14]. The same procedure was applied to the yellow/red ink, with the corresponding yellow and red states shown in Fig. 15. As with the white/red ink, the colours can be switched

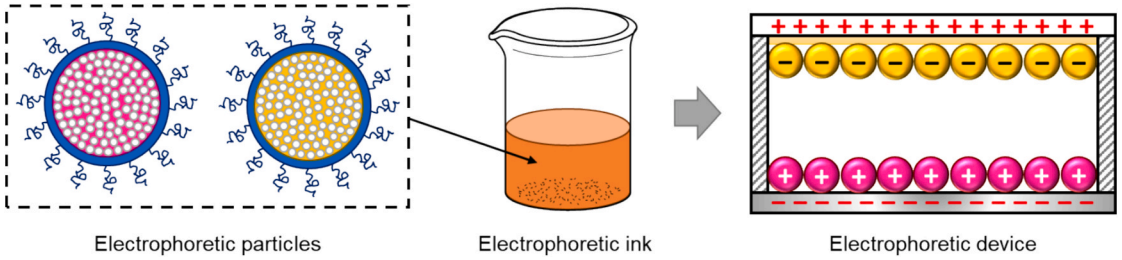

Fig. 13. Scheme of the yellow/red electrophoretic ink used in the electrophoretic device, displaying the yellow state.

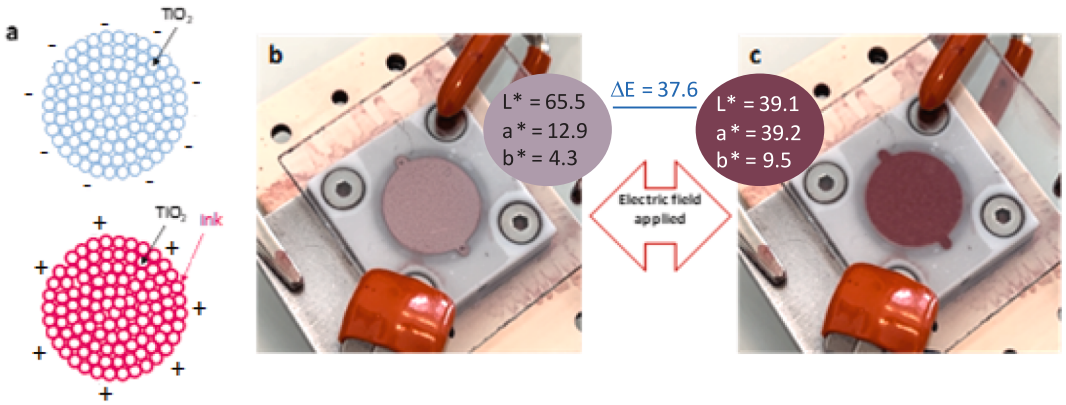

Fig. 14. A) scheme of the particles used to prepare the white/red electrophoretic inks, and corresponding prototype pixels in b) the white state and c) the red state. a video is associated with the file name: **red-white proto pixel.mov**.

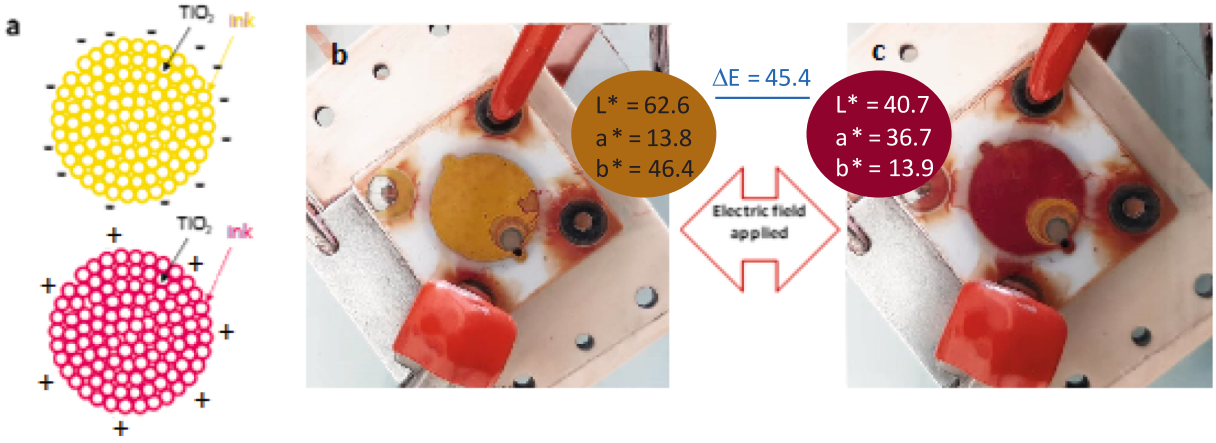

Fig. 15. A) scheme of the particles used to prepare the yellow/red electrophoretic inks, and prototype pixels in b) the yellow state and c) the red state.

repeatedly without any loss of contrast. For both prototype pixels, the colour coordinates of the two states and the colour difference between them are reported.

4. Conclusion

EPID technology has been widely adopted in e-paper applications due to its flexibility, low power consumption, and excellent visibility under sunlight. The success of monochromatic EPIDs has driven the development of full-colour EPIDs to meet the growing demand for this technology across various devices. Colour electrophoretic displays can be achieved through two in-competition approaches: colour filters and the multi-particle method. The multi-particle method offers the potential for high visual quality by combining high reflectivity with high contrast. However, a major limitation remains the lack of saturated, non-toxic, and primary-coloured inorganic pigments, which must be addressed to fully realize this method's potential. This article presents an innovative approach to the development of multicolour EPID devices—crucial for market expansion—through the design of hybrid particles that synergistically combine the advantages of inorganic pigments (high reflectivity, opacity, and voltage-responsive mobility) with those of organic dyes (bright cyan, magenta, and red colorations).

The hybrid pigment spheres consist in an inorganic TiO_2 core and a molecular dye (commercial cyan, magenta, or yellow ink), optionally encapsulated in a PMMA shell. These hybrid particles are specifically engineered to be charged for effective electrophoretic mobility, making them suitable for integration into pixel prototypes for full-colour EPIDs. The fabrication process involves several key steps.

(i) **Preparation of hybrid pigment spheres**. Varying amounts of organic inks (Epson) were added to aqueous suspensions of nanometric TiO_2 particles. Atomizing these suspensions resulted in vividly coloured spherical TiO_2 aggregates with saturated hues. By mixing cyan, magenta, and yellow hybrid pigments, a broad spectrum of colours can be achieved, which can be accurately predicted using Duncan-type mixing laws. Red, blue and green colours have been produced from the adequate mixings in order to validate the concept.

(ii) **Stability enhancement.** To address potential long-term stability issues caused by dye dissolution in Isopar G (a common EPID fluid), we initially considered introducing a water-soluble polymer (PAA or PVA) during the spray-drying process. However, this step proved unnecessary, as the TiO_2/ink hybrid pigment spheres obtained after spray-drying demonstrated colour stability in Isopar G over several months. Although long-term stability under UV irradiation and varying ambient temperatures remains to be demonstrated, the proof of concept is successfully established here.

(iii) **Functionalization.** To ensure stability in apolar media and facilitate particle movement under an electric field, the inorganic spheres underwent three functionalization steps: silanisation; encapsulation with an adequate polymer coating, and charge introduction via acid-base interactions between the polymer shells.

(iv) **Electrophoretic testing.** The functionalized electrophoretic particles were introduced into test cells to assess the contrast between negatively and positively charged hybrid particles on

the cell surface, forming what is known as a dual-colour display. Both white/red and yellow/magenta ink combinations displayed alternating surface colourations without any degradation in ΔE colour difference, allowing for multiple complete refresh cycles.

In conclusion, this research introduces a promising approach for developing multicolour EPID devices, with the potential to achieve a wider colour gamut than current full-colour EPID technologies. Future work in this area could focus on optimizing the colour-mixing system on the EPID screen, particularly by refining pixel composition and size. A key goal would be to manipulate surface charge levels to enable four-color pixel configurations. Additionally, effort could be directed toward fabricating and testing larger-scale full-colour EPID prototypes, exploring a wider range of colour combinations and their stability, and investigating methods to further enhance colour saturation and contrast, at the scale of prototype devices. By addressing these challenges, researchers could pave the way for the next generation of vibrant, energy-efficient, and versatile full-colour e-paper displays, expanding their applications across a variety of industries and devices.

Author Contributions

The manuscript was written through contributions of all authors. All authors have given approval to the final version of the manuscript. All authors contributed equally.

Funding Sources

This study was carried out with financial support of ANR program (ANR n° 20-CE09-0032 – DEFINED).

All the data (method, hardware, software, etc.) needed to reproduce our research are already well described/referenced in this article, so they are "shared".

CRediT authorship contribution statement

Lydia Muentz: Investigation. **Emile Decompte:** Investigation. **Hugo Ravet:** Investigation. **Nicolas Penin:** Writing – review & editing, Methodology, Conceptualization. **Anthony Chiron:** Methodology, Investigation. **Cyril Brochon:** Writing – review & editing, Project administration, Conceptualization. **Georges Hadziioannou:** Validation, Resources. **Elodie Bourgeat-Lami:** Writing – review & editing, Project administration, Funding acquisition. **Manuel Gaudon:** Writing – original draft, Supervision, Conceptualization.

Declaration of competing interest

The authors declare that they have no known competing financial interests or personal relationships that could have appeared to influence the work reported in this paper.

Appendix A. Supplementary data

Supplementary data to this article can be found online at https://doi.org/10.1016/j.matdes.2025.114563.

Data availability

No data was used for the research described in the article.

References

[1] B. Comiskey, J.D. Albert, H. Yoshizawa, J. Jacobson, An electrophoretic ink for all-printed reflective electronic displays, Nature 394 (1998) 253–255, https://doi.org/10.1038/28349.
[2] J.A. Rogers, Z. Bao, Printed plastic electronics and paperlike displays, J. Polym. Sci., Part A: Polym. Chem. 40 (2002) 3327–3334, https://doi.org/10.1002/pola.10405.
[3] S. Kholghi Eshkalak, M. Khatibzadeh, E. Kowsari, A. Chinnappan, W.A.D. M. Jayathilaka, S. Ramakrishna, Overview of electronic ink and methods of production for use in electronic displays, Opt. Laser Technol. 117 (2019) 38–51, https://doi.org/10.1016/j.optlastec.2019.04.003.
[4] P. Mürau, B. Singer, The understanding and elimination of some suspension instabilities in an electrophoretic display, J. Appl. Phys. 49 (1978) 4820–4829, https://doi.org/10.1063/1.325511.
[5] B.-R. Yang, W.-J. Hu, Z. Zeng, Z.-Y. Wu, Y.-F. Gu, J.-Z. Xu, J.-X. Cao, Y.-D. Zhang, P. Chen, Understanding the mechanisms of electronic ink operation, J. Soc. Inf. Disp. 29 (2021) 38–46, https://doi.org/10.1002/jsid.960.
[6] C.A. Kim, M.J. Joung, S.D. Ahn, G.H. Kim, S.-Y. Kang, I.-K. You, J. Oh, H. J. Myoung, K.H. Baek, K.S. Suh, Microcapsules as an electronic ink to fabricate colour electrophoretic displays, Synth. Met. 151 (2005) 181–185, https://doi.org/10.1016/j.synthmet.2005.03.00.
[7] S. Inoue, H. Kawai, S. Kanbe, T. Saeki, T. Shimoda, High-resolution microencapsulated electrophoretic display (EPID) driven by poly-Si TFTs with four-level grayscale, IEEE Trans. Electron Devices 49 (2002) 1532–1539, https://doi.org/10.1016/j.synthmet.2005.03.008.
[8] J.I. Choi, E. Sluzky, M. Anc, A. Piquette, M.E. Hannah, K.C. Mishra, J. McKittrick, J. B. Talbot, EPID of phosphors for display and solid-state lighting technologies, Key Eng. Mater. 507 (2012) 149–153, https://doi.org/10.4028/www.scientific.net/KEM.507.149.
[9] Q. Fan, Q. Luo, Z. Zhao, G. Zou, Z. Wu, Z. Zeng, Z. Qin, S. Deng, B.-R. Yang, Full-colour electrophoretic display with high halftone image quality, reduced power, and deep-learning-enabled fast implementation, Appl. Opt. 63 (2024) 8340–8349, https://doi.org/10.1364/AO.532573.
[10] H. Zang, C. Lin, M. Jalil, H. Gu, Y. Chen, A five-colour electrophoretic display, Proc. Int. Dis. Workshops 29 (2022) 802–805, https://doi.org/10.36463/idw.2022.0802.
[11] M. Jiang, Z. Yi, J. Wang, F. Li, B. Lai, L. Li, L. Wang, L. Liu, F. Chi, G. Zhou, Optimized driving scheme for three-colour electrophoretic displays based on the elimination of red ghost images, Micromachines 15 (2024) 1260, https://doi.org/10.3390/mi15101260.
[12] X. Wang, G. Li, X. Zeng, D. Hu, Y. Chen, 19.2: invited paper: driving and evaluating methods for color electronic paper, Symp Digest of Tech Papers 53 (2022) 230, doi: 10.1002/sdtp.15899.
[13] R. Fleming, S. Peruvemba, R. Holman, S. Ferguson, B. Sadlik, T. Johansson, 48-2: electronic paper 2.0: frustrated eTIR as a path to color and video, Symp Digest of Tech Papers 49 (2018) 630–632, https://doi.org/10.1002/sdtp.12402.
[14] Y. Zhang, D. Zeng, J. He, H. Sheng, T. Zhou, J. Shi, L. Peng, X. Wu, B.-R. Yang, High-performance multi-particle color electrophoretic display: a novel dual-charged particle strategy, Chem. Eng. J. 514 (2025) 163010, https://doi.org/10.1016/j.cej.2025.163010.
[15] X. Li, J. Zhao, H. Xiao, H. Zhang, M. Zhou, X. Zhang, X. Yan, A. Tang, L. Chen, Multiparticle synergistic electrophoretic deposition strategy for high-efficiency and high-resolution displays, ACS Nano 18 (2024) 17715–17724, https://doi.org/10.1021/acsnano.4c03005.
[16] Y. Zhang, J. Yang, F. Xiong, X. Wu, D. Zeng, T. Zhou, B. Yang, Coupling-grafting ultrasonication modification of electrophoretic particles for fast response and high contrast ratio electrophoretic display, Adv. Mater. Technol. 9 (2024) 2400029, https://doi.org/10.1002/admt.202400029.
[17] B. Peng, Y. Li, J. Li, L. Bi, H. Lu, J. Xie, X. Ren, Y. Cao, N. Wang, X. Meng, L. Deng, Z. Guo, Monodisperse light color nanoparticle ink toward chromatic electrophoretic displays, Nanoscale 8 (2016) 10917–10921, https://doi.org/10.1039/C6NR02524B.
[18] J. Cao, T. Hasegawa, Y. Asakura, P. Sun, S. Yang, B. Li, W. Cao, S. Yin, Synthesis and colour tuning of titanium oxide inorganic pigment by phase control and mixed-anion co-doping, Adv. Powder Technol. 33 (2022) 103576, https://doi.org/10.1016/j.apt.2022.103576.
[19] B. Serment, M. Gaudon, A. Demourgues, A. Noël, G. Fleury, E. Cloutet, G. Hadziioannou, C. Brochon, Cyan $Ni_{1-x}Al_{2+2x/3}\square_{x/3}O_4$ single-phase pigment synthesis and modification for electrophoretic ink formulation, ACS Omega 5 (2020) 18651–18661, https://doi.org/10.1021/acsomega.0c01289.
[20] S. Kimura, Y. Kaneko, K. Marumoto, Y. Suzuki, Synthesis and colour development mechanism of $Li_2CoTi_3O_8$ cyan pigments: effect of synthetic temperature, J. Ceram. 128 (2020) 260–266, https://doi.org/10.2109/jcersj2.20037.
[21] A. Verma, J. Li, M.A. Subramanian, Cr^{2+} in square planar coordination: durable and intense magenta pigments inspired by lunar mineralogy, Chem. Mater. 36 (2024) 3837–3843, https://doi.org/10.2109/jcersj2.20037.
[22] B. Serment, L. Corucho, A. Demourgues, G. Hadziioannou, C. Brochon, E. Cloutet, M. Gaudon, Tailoring the Chemical Composition of $LiMPO_4$ (M = Mg, Co, Ni) Orthophosphates to design new inorganic pigments from magenta to yellow hu, Inorg. Chem. 58 (2019) 7499–7510, https://doi.org/10.1021/acs.inorgchem.9b00715.
[23] P.K. Thejus, K.V. Krishnapriya, K.G. Nishanth, NIR reflective, anticorrosive magenta pigment for energy saving sustainable building coatings, Sol. Energy 222 (2021) 103–114, https://doi.org/10.1016/j.solener.2021.05.017.
[24] N. Gorodylova, P. Šulcová, Polymerizable precursor method vs solid state reaction for the synthesis of $Ni_3(PO_4)_2$ yellow hue pigment with advanced characteristics, J. Alloys Compd. 903 (2022) 163854, https://doi.org/10.1016/j.jallcom.2022.163854.
[25] J. Chen, Y. Xiao, B. Huang, X. Sun, Sustainable cool pigments based on iron and tungsten co-doped lanthanum cerium oxide with high NIR reflectance for energy saving, Dyes Pigm. 154 (2018) 1–7, https://doi.org/10.1016/j.jallcom.2022.16385 4.
[26] B. Bae, S. Tamura, N. Imanaka, Novel environment-friendly yellow pigments based on praseodymium(III) tungstate, Ceram. Int. 43 (2017) 7366–7368, https://doi.org/10.1016/j.ceramint.2017.02.10.

[27] M. Wang, C. Lin, H. Du, H. Zang, M. McCreary, 59.1: Electrophoretic Display Platform Comprising B, W, R Particles, SID Symp, Dig. Tech. Pap. Figures (2014) 857–860, https://doi.org/10.1002/j.2168-0159.2014.tb00226.x.
[28] S.J. Telfer, M.D. McCreary, 42-4: a full-color electrophoretic display, SID Symp. Dig. Tech. Pap. 47 (2016) 574–577, https://doi.org/10.1002/sdtp.10736.
[29] E. Huitema, I. French, E Ink's technicolor moment: the road to color E-paper took two decades, IEEE Spectr. 59 (2022) 30–35, https://doi.org/10.1109/MSPEC.2022.9706404.
[30] B. Rana, G.K. Joshi, Electrophoresis: basic principle, types and applications, in: A. K. Bhatt, R.K. Bhatia, T.C. Bhalla (Eds.), Basic Biotechniques for Bioprocess and Bioentrepreneurship, Academic Press, 2023, pp. 183–193.
[31] C.-M. Lu, C.-L. Wey, A Controller Design for Colour Active-Matrix Displays using Electrophoretic Inks and Colour Filters, J. Display Technol. 7 (2011) 482–489, https://doi.org/10.1109/JDT.2011.2141114.
[32] Y. Fang, J. Wang, L. Li, Z. Liu, P. Jin, C. Tang, Preparation of chromatic composite Hollow nanoparticles containing mixed metal oxides for full-colour electrophoretic displays, J. Mater. Chem. C 4 (2016) 5664–5670, https://doi.org/10.1039/c6tc01694d.
[33] H. Ravet, N. Penin, A. Chiron, C. Brochon, F. Brunel, M. Duttine, E. Bourgeat-Lami, M. Gaudon, Impact of harsh grinding on the structure and colour of $LiCoPO_4$ and $LiNiPO_4$ pigments, Inorg. Chem. 64 (2025) 166–180, https://doi.org/10.1021/acs.inorgchem.4c04406.
[34] M.D. Fairchild, Colour Appearance Models, in: Colour Appearance Models, John Wiley and Sons, 2013, pp. 199–212.
[35] R. Su, R. Bechstein, L. Sø, R.T. Vang, M. Sillassen, B. Esbjörnsson, A. Palmqvist, F. Besenbacher, How the anatase-to-rutile ratio influences the photoreactivity of TiO_2, J. Phys. Chem. C 115 (2011) 24287–24292.
[36] T. Ishigaki, Y. Nakada, N. Tarutani, T. Uchikoshi, Y. Tsujimoto, M. Isobe, H. Ogata, C. Zhang, D. Hao, Enhanced visible-light photocatalyticactivity of anatase-rutile mixed-phase nano-sizepowder given by high-temperature heat treatment, R.soc. Open Sci. 7 (2020) 191539, https://doi.org/10.1098/rsos.191539.
[37] J. Hong, M. Lai, J. Chen, L. Zhou, T. Sun, B. Ma, Y. Chen, X. Zeng, M. Wu, Dual-mode chromatic electrophoretic display: a prospective technology based on fluorescent electrophoretic particles, Chem. Eng. J. 439 (2022) 135726, https://doi.org/10.1016/j.cej.2022.135726.
[38] H. Yang, S. Zhu, N. Pan, N. On the Kubelka—Munk single-constant/two-constant theories, Text. Res. J. 80 (2010) 263–270. doi:10.1177/00405175080999.
[39] D.R. Duncan, The colour of pigment mixtures, Proc. Phys. Soc. 52 (1940) 390, https://doi.org/10.1088/0959-5309/52/3/310.
[40] L. Simonot, M. Hébert, Between additive and subtractive colour mixings: intermediate mixing models, J. Opt. Soc. Am. A 31 (2013) 58–66, https://doi.org/10.1364/JOSAA.31.000058.
[41] A. Noel, D. Mirbel, A. Charbonnier, E. Cloutet, G. Hadziioannou, C. Brochon, Synthesis of charged hybrid particles via dispersion polymerization in nonpolar media for color electrophoretic display application, J. Polym. Sci., Part A: Polym. Chem. 55 (2017) 338–348, https://doi.org/10.1002/pola.28393.
[42] A. Noel, D. Mirbel, E. Cloutet, G. Fleury, C. Schatz, C. Navarro, G. Hadziioannou, C. Brochon, Tridodecylamine, an efficient charge control agent in non-polar media for electrophoretic inks application, Appl. Surf. Sci. 428 (2018) 870–876, https://doi.org/10.1016/j.apsusc.2017.09.171.
[43] A.L. Dalisa, Electrophoretic display technology, IEEE Trans. Electron Devices 24 (1977) 827–834, https://doi.org/10.1109/T-ED.1977.18838.
[44] T. Bert, F. Beunis, H. De Smet, K. Neyts, Steady state current in EPIDs, Displays 27 (2006) 35–38, https://doi.org/10.1016/j.displa.2005.06.008.
[45] Y. Yu, H. Liu, Y. Zhen, Y. Liu, B. Gao, X. Li, S. Wang, Adjusting the charging behavior of TiO_2 with basic surfactants in an apolar medium for electrophoretic displays, Nanoscale Adv. 6 (2024) 4111–4118, https://doi.org/10.1039/d4na00301b.
[46] M. Badila, A. Hébraud, C. Brochon, G. Hadziioannou, Design of coloured multilayered electrophoretic particles for electronic inks, ACS Appl. Mater. Interfaces 3 (2011) 3602–3610, https://doi.org/10.1021/am200815a.